© 1973 IEEE. Personal use of this material is permitted. However, permission to reprint/republish this material for advertising or promotional purposes or for creating new collective works for resale or redistribution to servers or lists, or to reuse any copyrighted component of this work in other works must be obtained from the IEEE.

BEAM BREAKUP IN A 55-CELL SUPERCONDUCTING ACCELERATOR STRUCTURE*

K. Mittag†, H. A. Schwettman‡ and H. D. Schwarz

Department of Physics and High Energy Physics Laboratory

Stanford University
Stanford, California 94305

Introduction

Longitudinal and transverse beam breakup defines an upper limit to the beam current that can be attained in a linear accelerator.[1,2,3] In a superconducting accelerator (SCA), the problem of regenerative beam breakup is particularly important because the inherent Q-values of the relevant modes are extremely large. On the other hand, the problem of cumulative beam breakup in a SCA is comparable to that in a conventional electron linac.[4] In this paper we describe the regenerative beam breakup characteristics of the 55-cell multiperiodic structure which is the basic unit of the SCA being developed at Stanford.[5] The breakup characteristics of the capture section and the pre-accelerator section have been described previously.[4] In these studies it is demonstrated that the relevant breakup modes can be selectively loaded, and that the starting current for regenerative beam breakup in a SCA can be increased to 500 μA, a value well in excess of the initial design objective of 100 μA.

Passbands of the 55-Cell Structure

The basic unit of the SCA is a 55-cell multi-periodic structure of the iris loaded type. The structure is 8-cell periodic, and, as illustrated in Fig. 1, consists of seven sub-structures. The five long cells in the center of each sub-structure are $\lambda/2$ in length, whereas the short cells are about $\lambda/3$ in length, λ being the free space wavelength of the accelerator mode at a frequency of 1.3 GHz.

Regenerative beam breakup must be suppressed for the longitudinal TM_{01}-band and the transverse HEM_{11}-band. To determine the character of these bands, which are shown in Fig. 2, we have measured the resonant frequency of each mode and performed bead measurements to obtain field profiles. The effective wave number k of the individual modes are calculated from the expression $k = n\pi/L$. The effective length L of each mode, as well as its phase shift $n\pi$ over this length, were obtained by analyzing the bead measurements. The mutli-periodic character of the 55-cell structure leads to several unusual features in the TM_{01}-band and the HEM_{11}-band. First, the modes of the TE_{11}-like branch of the HEM_{11}-band are localized to the group of five long cells or to the group of short cells in each sub-structure. The reason for this is the strong dependence of the resonant frequency of a TE_{111}-mode on cell length. Second, because the structure is 8-cell periodic, the TM_{11}-like branch of the HEM_{11}-band is split into eight sub-bands. Third, the TM_{11}-like branch of the HEM_{11}-band is double-valued, as is observed in some separator structures.[6,7] This behaviour indicates that the coupling between cells changes from magnetic to electric as one moves from one end of the TM_{11}-like branch to the other, the magnitude of the coupling being relatively small near the minimum of the dispersion curve. Since the TE-admixture to the modes near the minimum is quite large and the coupling is small, it is not totally surprising that the modes at 1.742 GHz and 1.788 GHz, are localized to the five long cells of each sub-structure.

Because of fabrication errors in real structures, the rotational symmetry is broken and the two polarizations of the HEM_{11}-modes are no longer degenerate. The splitting between the two polarizations of the HEM_{11}-modes varies between 50 kHz and 500 kHz.

Experimental Determination of I_SQ_L-Values

The beam breakup characteristics of the 55-cell multi-periodic structure are summarized by the I_SQ_L-values of the individual modes of the TM_{01}-band and the HEM_{11}-band. I_S is the starting current for beam breakup in a mode where the loaded Q-value is Q_L. Measurement of the I_SQ_L-value is essential in order to determine the external loading necessary for suppression of beam breakup. In order to experimentally determine the I_SQ_L-value of a particular breakup mode, one excites this mode with an external generator, and measures the relative change in stored energy for this mode due to the exchange of energy between an electron beam and the electromagnetic fields. An 8 MeV electron beam from the superconducting injector, pulsed with a period of a few seconds, was employed in these measurements. The relative change in stored energy, the beam current, and the loaded Q-value of the mode are sufficient to determine the I_SQ_L-value.[4] The I_SQ_L-values for the first and second structures in the SCA are given in Table I. These I_SQ_L-values have been calculated from the experimentally determined values assuming a dependence on electron beam energy as theoretically predicted.[4,8]

External Loading of the Beam Breakup Modes

The inherent Q-values in a superconducting structure are quite high, and thus to achieve large average beam currents care must be exercised that all relevant breakup modes are externally loaded. Our objective is to load all breakup modes so that their starting currents are 500 μA or larger. Once this problem is solved for the first accelerator section, it is also solved for all subsequent sections because the starting current increases with increasing beam energy. Therefore, we shall describe the loading

*Work supported in part by the National Science Foundation and the Office of Naval Research.

†Present address: Institut fur Experimentelle Kernphysik, Karlsruhe, Germany

‡ Alfred P. Sloan Research Fellow.

of this section first, referring to Table I for the achieved total external loading.

TM_{01}-modes near the accelerator mode can cause longitudinal beam breakup. Every other mode in the TM_{01}-band will be loaded down to the same order of magnitude as the accelerator mode (number 49 in Table I) by the rf input probe which is located in the center of the structure. The modes number 50 and 52 in this band are loaded down selectively by 2 magnetic loop probes coupling to the azimuthal magnetic field H_θ at the outer circumference of the short cell between sub-structures 2 and 3 (Fig. 1). This cell is unexcited in the accelerator mode and the power coupled out of these probes will be 70 mW for a typical accelerating field of 3.3 MV/m.

Loading of the HEM_{11}-modes which can lead to transverse beam breakup is more complex. First of all, each HEM_{11}-mode has two polarizations, and thus two probes located about 90° apart in the azimuthal direction must be provided to insure that both polarizations are externally loaded. In addition, due to the complexity of the multi-periodic structure, the HEM_{11}-modes are divided into four groups of modes each of which must be loaded by a separate set of probes. The main problem in loading down the HEM_{11}-modes is that of achieving high selectivity, since one wants to load down the transverse breakup modes without coupling appreciable power out of the accelerator mode. The modes in the TE_{11}-like branch are the simplest to load down in this respect, since they exhibit strong radial electric field components, E_r, at the circumference of the structure and electrical probes coupling to E_r have a selectivity larger than 10^2. This implies that less than 1 mW per probe will be coupled out of the accelerator mode for a typical accelerating field of 3.3 MV/m. As shown in Fig. 1, these loading probes have to be provided in each sub-structure because the TE_{11}-like modes are trapped in sub-structures. The same is true for the TM_{11}-like modes at 1.742 GHz, which also are localized in sub-structures. These modes are the most difficult to load down selectively because their fields at the outer circumference of the structure in the center of the cells are similar to those of the accelerator mode. For this set of modes magnetic loop probes coupling to H_θ are used, and a band-stop filter which rejects power coupled out of the accelerator mode at 1300 MHz is used to achieve selectivity. With the band-stop filter, described in the following section of this paper, 35 mW of power is coupled out for a typical accelerating field of 3.3 MV/m.

The third group of modes which require special loading probes are the TM_{11}-like modes number 36 through 41. These modes have very small field amplitudes in the long cells of each sub-structure, but have strong fields in the three short cells between sub-structures. These modes will be loaded down sufficiently by the two loading probes in the unexcited cell between sub-structures 2 and 3 (Fig. 1), which were described already.

The fourth group of modes are the TM_{11}-like modes number 1 through 35. These modes couple strongly enough to the TE_{11}-cut-off mode in the beam pipe, that they can be loaded by two magnetic loop probes coupling to the H_z-component of this cut-off mode at the outer circumference of the beam pipe (see Fig. 1). Band-stop filters are also used here and the power coupled out of one of these filters will be 10 mW under typical accelerating conditions.

The total power coupled out of all loading probes will be about 600 mW for the first accelerator structure. We can afford to dump this power into the helium bath, and thus the probes are terminated at helium temperatures with 50 Ω loads.

The second and all subsequent accelerator structures will have identical sets of loading probes. Table I lists the $I_S Q_L$-values, the loading probes and the achieved total external loading for the second structure. Compared to the first structure, the loading in the second one is simplified by loading the TE_{11}-like modes and the TM_{11}-like modes at 1.742 GHz with the same set of magnetic loading probes in each sub-structure. The plane of these loops will be oriented at 45° with respect to the axis of the accelerator. Therefore, such a probe will couple both to the H_z-component of the TE_{11}-like modes and to the H_θ-component of the TM_{11}-like modes. A total of 340 mW will be dissipated in the helium bath by terminating all probes of the second structure at helium temperature.

Description and Performance of the Band-Stop Filter

The purpose of the band-stop filter[9] is to reject the power coupled out of the accelerator mode at 1.3 GHz without affecting the coupling at the frequencies of the breakup modes which lie between 1.5 and 1.9 GHz. This can be achieved by shunting the output of the loop probes with a resonant circuit in the form of a shorted coaxial line, $\lambda/2$ in length, λ being the wavelength coresponding to the accelerator mode frequency. The design of a filter based on this principle is illustrated in Fig. 3.

The width of the stopband can be chosen within limits by the characteristic impedance of the resonant line. An impedance of 28 Ω was found to be optimal. The position of the shunt relative to the coupling loops is important and has to be approximately $\lambda/4$. Under this condition the wave travelling into the filter is reduced by a factor of 2 in the ideal lossless case compared to a wave excited by a loop probe with no filter. This increases the attenuation of the filter by 6 dB and reduces the power dissipated in it. An impedance transformer between the shunt and the loop increase the coupling for the breakup modes. The length of this transformer is one quarter wavelength at approximately 1.7 GHz and its characteristic impedance is 28 Ω. The 50 Ω output line connected to the shunt is thus transformed to a low impedance at the loop, which increases the loading by 5 dB. The shunt at these higher frequencies has changed to high impedance and does not affect the wave propagation much.

In order to minimize the rf-losses at helium temperature, the filter is built out of niobium. The performance of a filter at room temperature is shown in Fig. 4. The maximum attenuation is 46 dB, and the Q-value is about 300 for the resonant stub. For an improvement factor of 10^3 for the superconducting filter compared to the normal conducting version, the rf-losses at helium temperature should be smaller than 1 mW for 100 watts of power coupled into it at 1.3 GHz.

In an experiment employing a superconducting cavity resonant at 1.3 GHz, a niobium filter was tested in its superconducting state. Measuring the Q-value of the cavity as a function of field level, we observed that the filter turned normal at an accelerating electric field of 4.7 MV/m. Taking into account that our test filter was 0.38 cm nearer to the cavity surface than the analogous filters in the

accelerator structure will be, we can predict that in the accelerator the filters will turn normal conducting at an accelerating electric field of about 20 MV/m. Therefore, the filters certainly will not limit the maximum attainable accelerating field in a structure.

Conclusion

During tests with the SCA average beam currents up to 290 μA have been accelerated, although some of the loading probes indicated above had not yet been installed. With the full complement of loading probes, beam currents up to 500 μA with a duty factor of 1 should be attainable in the superconducting electron accelerator.

Acknowledgements

The authors wish to express their graditude to the staff of the High Energy Physics Laboratory for their tremendous effort in preparing for and conducting the tests of the cryogenic injector. Also, the support of M. S. McAshan, L. R. Suelzle, and J. P. Turneaure is very much appreciated, especially in designing various components of the system.

References

1. R. H. Helm and G. A. Loew, "Beam Breakup" in Linear Accelerators (P, M. Lapostolle and A. L. Septier, eds.) North Holland Pub. Co. (1970).

2. P. B. Wilson, "Theory and Design of Superconducting Electron Accelerators", ibid.

3. A. Citron and H. Schopper, "Superconducting Proton Linear Accelerators and Particle Separators", ibid.

4. K. Mittag, H. A. Schwettman and H. D. Schwarz, Proc. of the 1972 Proton Linear Accelerator Conf., Los Alamos, Oct. 1972.

5. M. S. McAshan, H. A. Schwettman, L. R. Suelzle and J. P. Turneaure, High Energy Physics Laboratory Report No. 665, Stanford University (1972).

6. B. W. Montague, "Radiofrequency Separators" in Linear Accelerators (P. M. Lapostolle and A. L. Septier, eds.) North Holland Pub. Co., (1970).

7. G. Saxon, T. R. Jarvis and I. White, Proc. IEEE 10, 1365 (1963).

8. P. B. Wilson, High Energy Physics Laboratory Report No. 297, Stanford University (1963).

9. G. L. Matthaei, L. Young and E.M.T. Jones, "Microwave Filters, Imedpance Matching Networks, and Coupling Structures", McGraw Hill (1964).

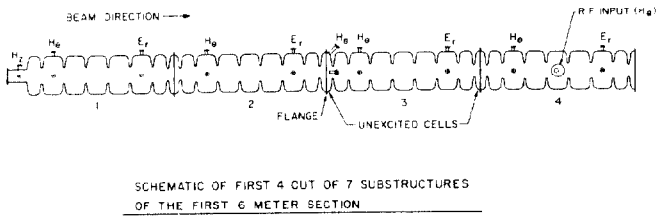


Fig. 1. Schematic of four sub-structures of the 55-cell accelerator section showing location and type of loading probes to suppress beam breakup.

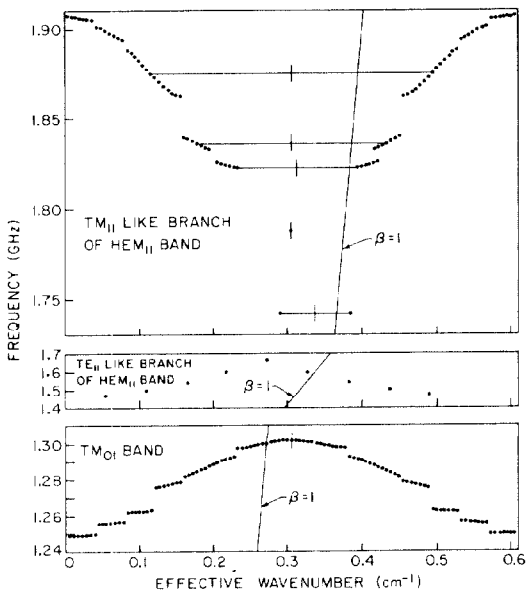


Fig. 2. Lowest passbands of the 55-cell accelerator section.

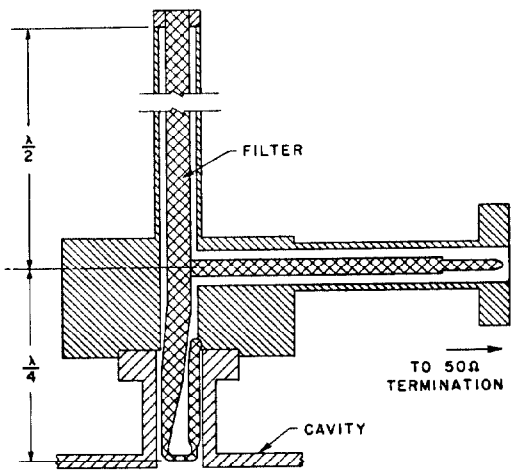


Fig. 3. Schematic of band-stop filter.

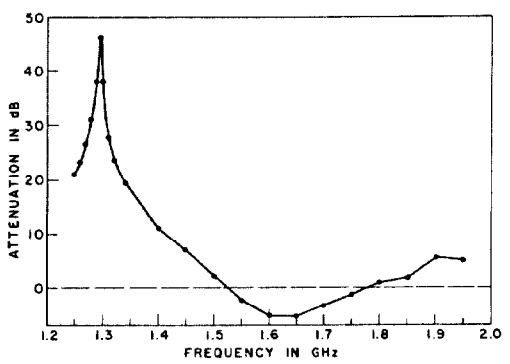


Fig. 4. Reduction of output power from loop probe by means of a band-stop filter.

TABLE I

BEAM BREAKUP PROPERTIES OF FIRST AND SECOND 55-CELL STRUCTURES

			First structure			Second structure		
Band*	N†	f(MHz)‡	$I_S Q_L$ (10^4A)	Probe**	Q_{ext} (10^7)	$I_S Q_L$ (10^4A)	Probe**	Q_{ext} (10^7)
TM_{01}	42	1297.506	-	-	-	-	-	-
"	43	1297.625	> 770	input	150	> 22,000	input	150
"	44	1297.920	< 0	-	-	< 0	-	-
"	45	1298.353	< 0	input	8	< 0	input	8
"	46	1298.806	< 0	-	-	< 0	-	-
"	47	1299.284	< 0	input	4	< 0	input	4
"	48	1299.745	< 0	-	-	< 0	-	-
"	49	1299.994	-	input	1	-	input	1
"	50	1300.691	> 100	H_θ(S)	80	> 1400	H_θ(S)	80
"	51	1301.000	> 12	input	6	> 160	input	6
"	52	1301.232	> 360	H_θ(S)	470	> 5000	H_θ(S)	470
"	53	1301.495	> 30	input	4	> 400	input	4
"	54	1301.622	< 0	-	-	< 0	-	-
"	55	1301.847	> 13	input	2	> 180	input	2
TE_{11}(1)	1	1470.666	> 300	E_r	70	> 900	H_z(L)	500
" (1)	2	1499.406	> 70	E_r	10	> 210	"	74
" (1)	3	1542.625	> 50	E_r	5	> 150	"	37
" (1)	4	1599.236	9	E_r	5	27	"	37
" (1)	5	1660.242	< 0	-	-	< 0	-	-
TM_{11}	1	1907.660	-	H_z(BP)	77	-	H_z(BP)	77
"	2	1907.466	-	"	21	-	"	21
"	3	1907.103	> 240	"	6.3	> 480	"	6.3
"	4	1906.665	> 160	"	6.5	> 320	"	6.5
"	5	1906.151	> 200	"	10	> 400	"	10
"	6	1905.677	> 240	"	10	> 480	"	10
"	7	1905.213	> 200	"	8	> 400	"	8
"	8	1901.707	> 100	"	14	> 200	"	14
"	9	1900.836	76	"	7	150	"	14
"	10	1899.497	< 0	"	5	< 0	"	5
"	11	1898.105	17	"	4	37	"	4
"	12	1896.455	17	"	5	37	"	5
"	13	1895.128	< 0	"	1.5	< 0	"	1.5
"	14	1894.250	< 0	"	6	< 0	"	6
"	15	1888.787	< 0	"	6	< 0	"	6
"	16	1886.977	> 50	"	3	> 100	"	3

* (1) refers to number of substructure in 6 m structure (See Fig. 1).

† mode number

‡ frequency of only one polarization

** probe which loads mode down to Q_{ext} ;
input, H_θ , H_z , E_r label both loading probes and fields to which probes couple;
L , S refer to long and short cells, BP to beam pipe (See Fig. 1).

TABLE I (Continued)

Band*	N†	f(MHz)‡	First structure $I_S Q_L$ (10^4A)	Probe**	First structure Q_{ext} (10^7)	Second structure $I_S Q_L$ (10^4A)	Probe**	Second structure Q_{ext} (10^7)
TM_{11}	17	1884.751	< 0	H_z(BP)	1.5	< 0	H_z(BP)	1.5
"	18	1882.466	> 80	"	2.2	> 170	"	2.2
"	19	1880.085	> 38	"	1.1	> 80	"	1.1
"	20	1877.543	> 58	"	1.8	> 120	"	1.8
"	21	1874.822	> 200	"	6	> 430	"	6
"	22	1872.730	> 42	"	1.8	> 90	"	1.8
"	23	1870.310	98	"	1.1	210	"	1.1
"	24	1867.894	< 0	"	2	< 0	"	2
"	25	1865.902	65	"	0.8	130	"	0.8
"	26	1864.123	< 0	"	1.4	< 0	"	1.4
"	27	1863.088	1.1	"	1.4	2.5	"	1.4
"	28	1862.509	- 2.8	"	2.5	< 0	"	2.5
"	29	1839.228	42	"	3	90	"	3
"	30	1838.309	- 2.8	"	3	< 0	"	3
"	31	1837.071	3.6	"	7	7.7	"	7
"	32	1835.749	- 4.4	"	13	< 0	"	13
"	33	1834.438	5	"	6	11	"	6
"	34	1833.345	- 5	"	10	< 0	"	10
"	35	1832.925	14	"	11	30	"	11
"	36	1825.754	> 0.16	H_θ(S)	< 0.5	> 0.4	H_θ(S)	< 0.5
"	37	1824.868	> 0.3	"	< 1.1	> 1	"	< 1.1
"	38	1824.241	> 0.3	"	< 0.35	> 1	"	< 0.35
"	39	1823.355	< 0	"	< 17	< 0	"	< 17
"	40	1822.758	< 0	"	< 3	< 0	"	< 3
"	41	1822.290	0.25	"	< 0.25	0.5	"	< 0.25
" (1)	42	1741.495	19	H_θ(L)	8	> 53	H_θ(L)	50
" (2)	43	1742.237	24	"	8	> 53	"	50
" (3)	44	1741.306	30	"	8	> 53	"	50
" (4)	45	1741.201	36	"	8	> 53	"	50
" (5)	46	1742.274	41	"	8	> 53	"	50
" (6)	47	1741.583	47	"	8	> 53	"	50
" (7)	48	1741.340	53	"	8	> 53	"	50
" (1)	49	1788.000	< 0	-	-	< 0	-	-
" (2)	50	1788.000	< 0	-	-	< 0	-	-
" (3)	51	1788.000	< 0	-	-	< 0	-	-
" (4)	52	1788.000	< 0	-	-	< 0	-	-
" (5)	53	1788.000	< 0	-	-	< 0	-	-
" (6)	54	1788.000	< 0	-	-	< 0	-	-
" (7)	55	1788.000	< 0	-	-	< 0	-	-